

Laplacian-level density functionals for the exchange-correlation energy of low-dimensional nanostructures

S. Pittalis^{1,*} and E. Räsänen^{2,†}

¹*Department of Physics and Astronomy, University of Missouri, Columbia, Missouri 65211, USA*

²*Nanoscience Center, Department of Physics, University of Jyväskylä, FI-40014 Jyväskylä, Finland*

(Dated: September 23, 2010)

In modeling low-dimensional electronic nanostructures, the evaluation of the electron-electron interaction is a challenging task. Here we present an accurate and practical density-functional approach to the two-dimensional many-electron problem. In particular, we show that spin-density functionals in the class of meta-generalized-gradient approximations can be greatly simplified by reducing the explicit dependence on the Kohn-Sham orbitals to the dependence on the electron spin density and its spatial derivatives. Tests on various quantum-dot systems show that the overall accuracy is well preserved, if not even improved, by the modifications.

PACS numbers: 71.15.Mb, 31.15.E-, 73.21.La

I. INTRODUCTION

With the present technology the electron gas can be confined in various ways to create nanoscale devices of lower dimension. The field of two-dimensional (2D) physics has grown rapidly alongside the development of electronic devices such as quantum Hall bars and point contacts, and semiconductor quantum dots. When modeling these systems, the finite extent in the growth direction (say z) can often be neglected, so that the system is well described by a 2D Hamiltonian in the effective-mass approximation.¹ In this respect, the building block is the 2D electron gas (2DEG), whose properties are well known in the literature.²

Density-functional theory (DFT) and its extensions have become the method of choice to describe the electronic properties of three-dimensional (3D) systems such as atoms, molecules and solids.^{3,4} Despite the fact that the many 3D density functionals developed for the exchange-correlation (xc) energy and potential fail in the quasi-2D limit,^{5–8} the derivation of *explicitly 2D* xc functionals has started only very recently.^{9–17} In finite 2D systems, most of these functionals overperform the 2D local spin-density approximation (LSDA), which is a combination of the analytic exchange energy of the 2DEG¹⁸ and the corresponding correlation energy having a parametrized form.^{19,20} The encouraging results obtained with the new functionals indicate that DFT in 2D has entered in a more mature phase.

Among the newly proposed functionals, our focus is on those approximations that have as ingredients the electron density and its spatial derivatives, the kinetic energy density and the paramagnetic current.^{9–15} In other words, the expressions of these functionals are current-dependent meta-generalized-gradient approximations (meta-GGAs), and therefore they explicitly depend on the Kohn-Sham (KS) orbitals. As it is valid for 3D systems, also for 2D systems the meta-GGAs are very accurate. However, the price for their accuracy is the more involved numerical implementation (if applied

self-consistently) as well as the (case-dependent) numerical burden in the applications. In order to simplify both the mentioned tasks, we explore here to which extent and how the explicit dependence on the KS orbitals may be reduced to the dependence on the electron density and its spatial derivatives, yet possibly maintaining a satisfactory level of accuracy. In other words, we examine the path *from implicit to explicit* density functionals in the class of meta-GGAs. A similar study has been already carried out for 3D systems, introducing some Laplacian-level meta-GGA functionals.²¹ With the present work, we explore this possibility for low-dimensional systems. We find that the performance after the simplifications is well preserved, and in some cases even improved.

II. REVIEW AND MODIFICATIONS OF THE FUNCTIONALS

In the following, we review the main ingredients of recently derived functionals and suggest how their expressions may be significantly simplified in a consistent fashion. Ideally, the ultimate goal is to obtain the best performance with the least (numerical) effort. In particular, we consider (i) an exchange-energy functional obtained through the modeling of the exchange-hole (x-hole) functions,⁹ (ii) an exchange-energy functional obtained from the one-body-density-matrix¹¹ (1BSDM), and (iii) correlation-energy functionals obtained through the modeling of the correlation hole.^{12,13} Details of the derivation of the functionals can be found in the mentioned literature.

A. Exchange energy from the exchange-hole functions

The exchange energy E_x can be expressed through the x-hole functions as^{3,4} $h_x^\sigma(\mathbf{r}_1, \mathbf{r}_2)$

$$E_x = \frac{1}{2} \sum_{\sigma} \int d^2r \rho_{\sigma}(\mathbf{r}) \int_0^{\infty} ds \int_0^{2\pi} d\phi_s h_x^{\sigma}(\mathbf{r}, \mathbf{r}+\mathbf{s}), \quad (1)$$

with

$$h_x^{\sigma}(\mathbf{r}_1, \mathbf{r}_2) = - \frac{|\sum_{k=1}^{N_{\sigma}} \psi_{k,\sigma}^*(\mathbf{r}_1) \psi_{k,\sigma}(\mathbf{r}_2)|^2}{\rho_{\sigma}(\mathbf{r}_1)}, \quad (2)$$

where $\psi_{k\sigma}(\mathbf{r})$ are the KS (spin) orbitals. From Eq. (1), it is apparent that an approximation of the x-hole also provides an approximation for the exchange energies. Equation (1) also suggests that the details of the angular dependence of the x-hole are energetically negligible: all we need is the *cylindrical* average of the x-hole, *i.e.* $\bar{h}_x^{\sigma}(\mathbf{r}; s)$.

As the basis of our model,⁹ we have chosen

$$\begin{aligned} \bar{h}_x^{\sigma}(\mathbf{r}; s) &= \frac{1}{2\pi} \int_0^{2\pi} d\phi_s h_x^{\sigma}(\mathbf{r}; \mathbf{r}+\mathbf{s}) \\ &\approx -\frac{a}{\pi} \exp[-a(\mathbf{r})(b(\mathbf{r})+s^2)] \\ &\times I_0\left(2a(\mathbf{r})\sqrt{b(\mathbf{r})s}\right), \end{aligned} \quad (3)$$

where $I_0(x)$ is the zeroth-order modified Bessel function of the first kind. This model provides the correct sign of the x-hole and the correct normalization $\int d^2s h_x^{\sigma}(\mathbf{r}, \mathbf{s}) = -1$. The non-negative functions $a(\mathbf{r})$ and $b(\mathbf{r})$ are introduced to reproduce the short-range behavior of the x-hole. It is important to note that the curvature of the x-hole in 2D is given by⁹

$$C_x^{\sigma}(\mathbf{r}) = \frac{1}{4} \left[\nabla^2 \rho_{\sigma}(\mathbf{r}) - 2\tau_{\sigma}(\mathbf{r}) + \frac{1}{2} \frac{(\nabla \rho_{\sigma}(\mathbf{r}))^2}{\rho_{\sigma}(\mathbf{r})} + 2 \frac{\mathbf{j}_{p,\sigma}^2(\mathbf{r})}{\rho_{\sigma}(\mathbf{r})} \right], \quad (4)$$

where τ_{σ} is (twice) the spin-dependent kinetic-energy density, and $\mathbf{j}_{p,\sigma}$ is the spin-dependent paramagnetic current density.

In Ref. 9, we have applied the above scheme in two ways. In the first instance, we have employed it in its full spirit by numerically determining a and b at each point in space. Then, in a fully self-consistent application, the scheme should be implemented within the optimized-effective-potential (OEP) method.^{22–26} This is necessary because τ_{σ} and $\mathbf{j}_{p,\sigma}$ (in non-current-spin-density functional calculations^{27,28}) make the overall scheme explicitly dependent on the KS orbitals. As a consequence, the corresponding numerical task would be highly nontrivial.

In the second instance, we have analyzed the 2DEG limit, for which

$$C_x^{\sigma}(\mathbf{r}) \rightarrow C_{h,x}^{\sigma}(\mathbf{r}) = -\pi \rho_{\sigma}^2(\mathbf{r}). \quad (5)$$

In this way, a *local* density functional has been recovered, which was seen to improve over the exchange energies

obtained within the standard LSDA when applied to few-electron quantum dots.

Next we proceed from the review of the functional to its modification. As discussed above, the task is to remove the explicit reference to the KS orbitals, yet retaining some degree of flexibility in dealing with inhomogeneous systems. This may be achieved by introducing the following modification:^{15,29,30}

$$\tau_{\sigma}(\mathbf{r}) = \sum_{k=1}^{N_{\sigma}} \psi_{k\sigma}(\mathbf{r}) \rightarrow \tilde{\tau}_{\sigma}(\mathbf{r}) = 2\pi \rho_{\sigma}^2(\mathbf{r}) + \frac{1}{3} \nabla^2 \rho_{\sigma}(\mathbf{r}) + \frac{\mathbf{j}_{p,\sigma}^2(\mathbf{r})}{\rho_{\sigma}(\mathbf{r})}. \quad (6)$$

Correspondingly, we obtain

$$C_x^{\sigma}(\mathbf{r}) \rightarrow \tilde{C}_x^{\sigma}(\mathbf{r}) = -\pi \rho_{\sigma}^2(\mathbf{r}) + \frac{1}{12} \nabla^2 \rho_{\sigma}(\mathbf{r}) + \frac{1}{8} \frac{(\nabla \rho_{\sigma}(\mathbf{r}))^2}{\rho_{\sigma}(\mathbf{r})}. \quad (7)$$

It is worth mentioning that due to the last (current-dependent) term on the right hand side of Eq. (6), the modified x-hole curvature manifestly preserves its gauge invariance. As described in Ref. 9, the functions a and b are determined from

$$a = \pi \rho_{\sigma} \exp(y), \quad (8)$$

and

$$b = \frac{y}{\pi \rho_{\sigma}} \exp(-y) \quad (9)$$

where $y = ab$ satisfies

$$(y-1) \exp(y) = \frac{\tilde{C}_x^{\sigma}}{\pi \rho_{\sigma}^2} = -1 + \frac{1}{12\pi} \frac{\nabla^2 \rho_{\sigma}}{\rho_{\sigma}^2} + \frac{1}{8\pi} \frac{(\nabla \rho)^2}{\rho_{\sigma}^3}. \quad (10)$$

If a solution does not exist, we set⁹ $y \equiv 0$. This corresponds to the 2DEG limit mentioned just above. From Eq. (10), it is apparent that the second and third terms are relevant when the curvature and the gradient of the spin-density are non-negligible.

Going back to the first modification $\tau_{\sigma} \rightarrow \tilde{\tau}_{\sigma}$, we refer to the new (angular-averaged) x-hole function as $\tilde{h}_x^{\sigma}(\mathbf{r}, s)$. The corresponding x-hole potentials denoted as $\tilde{U}_{x,\text{model}}^{\sigma}(\mathbf{r})$, read as follows⁹

$$\tilde{U}_{x,\text{model}}^{\sigma}(\mathbf{r}) = 2\pi \int_0^{\infty} ds \tilde{h}_x^{\sigma}(\mathbf{r}, s) \quad (11)$$

from which, the exchange energy is obtained as

$$\tilde{E}_x^{\text{model}} = \frac{1}{2} \sum_{\sigma} \int d^2r \rho_{\sigma}(\mathbf{r}) \tilde{U}_x^{\sigma}(\mathbf{r}). \quad (12)$$

The last two quantities calculated *without* the modification of τ_{σ} are denoted below simply without the tilde symbols, *i.e.*, $U_{x,\text{model}}^{\sigma}$ and $E_{x,\text{model}}^{\sigma}$.

Finally, we point out that the above modifications offer a straightforward way to calculate the corresponding KS exchange potential as a functional derivative, $v_x^{\sigma} = \delta \tilde{E}_x / (\delta \rho_{\sigma})$. The properties and performance of these potentials will be assessed elsewhere.

B. Exchange energy from the one-body-spin-density matrix

Another way to express the exchange energy is to make use of the 1BSDM $\gamma_\sigma(\mathbf{r}_1, \mathbf{r}_2)$,^{3,4} so that

$$E_x = -\frac{1}{2} \sum_{\sigma=\uparrow,\downarrow} \int d^2r \int_0^\infty ds \times \int_0^{2\pi} d\phi_s \left| \gamma_\sigma \left(\mathbf{r} + \frac{\mathbf{s}}{2}, \mathbf{r} - \frac{\mathbf{s}}{2} \right) \right|^2 \quad (13)$$

with

$$\gamma_\sigma(\mathbf{r}_1, \mathbf{r}_2) = \sum_{k=1}^{N_\sigma} \psi_{k,\sigma}(\mathbf{r}_1) \psi_{k,\sigma}^*(\mathbf{r}_2), \quad (14)$$

where $\psi_{k\sigma}(\mathbf{r})$ are the KS (spin) orbitals. Clearly, an approximation for the 1BSDM implies an approximation for the exchange energy. Also, it is apparent that the angular dependence of the 1BSDM is energetically of minor importance. Therefore, as a basis of our approximation we have considered the following expression¹¹

$$\frac{1}{2\pi} \int_0^\infty d\phi_s \left| \gamma_\sigma \left(\mathbf{r} + \frac{\mathbf{s}}{2}, \mathbf{r} - \frac{\mathbf{s}}{2} \right) \right|^2 \approx \rho_\sigma^2(\mathbf{r}) e^{-\frac{s^2}{\beta_\sigma(\mathbf{r})}} \times \left\{ 1 + \left[\frac{s}{\beta_\sigma(\mathbf{r})} \right]^2 A_\sigma(N_\sigma) \right\}, \quad (15)$$

where $\beta(\mathbf{r})$ is chosen to reproduce the exact-short behavior of the 1BSDM

$$\beta_\sigma^{-1}(\mathbf{r}) = \frac{1}{2} \frac{\tau_\sigma(\mathbf{r})}{\rho_\sigma(\mathbf{r})} - \frac{1}{8} \frac{\nabla^2 \rho_\sigma(\mathbf{r})}{\rho_\sigma(\mathbf{r})} - \frac{1}{2} \left(\frac{\mathbf{j}_{p,\sigma}(\mathbf{r})}{\rho_\sigma(\mathbf{r})} \right)^2 \quad (16)$$

and $A_\sigma(N_\sigma)$ is obtained through the normalization of the particle number for each spin channel. In Ref. 11 we have employed this scheme leading to accurate results for various quantum-dot systems. In addition, we have observed that this approach and the one of Sec. II A coincide in the 2DEG limit.

Here we suggest to simplify the present functional by making use of Eq. (6) in Eq. (16). This yields

$$\tilde{\beta}_\sigma^{-1}(\mathbf{r}) = \pi \rho_\sigma(\mathbf{r}) + \frac{1}{24} \frac{\nabla^2 \rho_\sigma(\mathbf{r})}{\rho_\sigma(\mathbf{r})}. \quad (17)$$

We emphasize that no gradients of the spin-density appear in this expression. The resulting expression is manifestly gauge invariant. The relevance of the gauge invariance of the expression in Eq. (16) has been already verified in Ref. 11. The final expression reads as

$$\tilde{E}_x^{\text{1BSDM}} = -\frac{\pi}{2} \sum_{\sigma=\uparrow,\downarrow} \int d^2r \left[\sqrt{\pi} + \frac{3}{4} \tilde{A}_\sigma \right] \times \rho_\sigma^2(\mathbf{r}) \tilde{\beta}_\sigma^{1/2}(\mathbf{r}), \quad (18)$$

where \tilde{A}_σ is determined through the normalization as

$$N_\sigma = \pi \int d^2r \left[1 + 2\tilde{A}_\sigma \right] \rho_\sigma^2(\mathbf{r}) \tilde{\beta}_\sigma(\mathbf{r}). \quad (19)$$

Equation (18) together with Eq. (19) provide another density functional for the exchange energy. Finally, the x-hole potential has a form

$$\tilde{U}_{x,\text{1BSDM}}^\sigma(\mathbf{r}) = -\pi \left[\sqrt{\pi} + \frac{3}{4} \tilde{A}_\sigma \right] \rho_\sigma(\mathbf{r}) \tilde{\beta}_\sigma^{1/2}(\mathbf{r}). \quad (20)$$

Similarly to the previous section, the exchange-hole potentials and exchange energies calculated *without* the modification of τ_σ are denoted below simply without the tilde symbols, i.e., $U_{x,\text{1BSDM}}^\sigma$ and $E_{x,\text{1BSDM}}^\sigma$.

C. Correlation energy from the correlation-hole functions

High predictive power in the application of DFT requires the accurate treatment of the electronic correlation in both inhomogeneous systems and in the limit of the homogeneous electron gas. We have achieved this goal in 2D by generalizing our previous approximation¹² to a parameter-free form,¹³ which reproduces the correlation energy of the 2DEG while preserving the ability to deal with inhomogeneous systems (quantum dots).

The correlation energy is expressed in terms of the cylindrical average of the (coupling-constant dependent) correlation-hole (c-hole) functions $\bar{h}_{c,\lambda}^{\sigma\sigma'}(\mathbf{r}, s)$ as follows:^{3,4}

$$E_c^{\sigma\sigma'} = \pi \int d\mathbf{r} \rho_\sigma(\mathbf{r}) \int_0^\infty ds \int_0^1 d\lambda \bar{h}_{c,\lambda}^{\sigma\sigma'}(\mathbf{r}, s). \quad (21)$$

It is obvious that an approximation for $\bar{h}_{c,\lambda}^{\sigma\sigma'}(\mathbf{r}, s)$ implies an approximation for $E_c^{\sigma\sigma'}$. In modeling these quantities, we have proposed a form¹²

$$\bar{h}_{c,\lambda}^{\sigma\sigma}(\mathbf{r}, s) \approx \frac{2\lambda s^2}{3} \left[\frac{(s - z_{\sigma\sigma}(\mathbf{r})) D_\sigma(\mathbf{r})}{1 + \frac{2}{3}\lambda z_{\sigma\sigma}(\mathbf{r})} \right] \exp\left(-\frac{9\pi s^2}{16z_{\sigma\sigma}^2(\mathbf{r})}\right) \quad (22)$$

$$\bar{h}_{c,\lambda}^{\sigma\bar{\sigma}}(\mathbf{r}, s) \approx 2\lambda \rho_{\bar{\sigma}}(\mathbf{r}) \left[\frac{s - z_{\sigma\bar{\sigma}}(\mathbf{r})}{1 + 2\lambda z_{\sigma\bar{\sigma}}(\mathbf{r})} \right] \exp\left(-\frac{\pi s^2}{4z_{\sigma\bar{\sigma}}^2(\mathbf{r})}\right) \quad (23)$$

for the same- and opposite-spin cases, $\sigma\sigma' = \sigma\sigma$ and $\sigma\sigma' = \sigma\bar{\sigma}$, respectively. Here

$$D_\sigma(\mathbf{r}) := \frac{1}{2} \left(\tau_\sigma - \frac{1}{4} \frac{(\nabla \rho_\sigma)^2}{\rho_\sigma} - \frac{\mathbf{j}_{p,\sigma}^2}{\rho_\sigma} \right) \quad (24)$$

and

$$z_{\sigma\sigma}(\mathbf{r}) := 2c_{\sigma\sigma} |U_x^\sigma(\mathbf{r})|^{-1}, \quad (25)$$

$$z_{\sigma\bar{\sigma}}(\mathbf{r}) := c_{\sigma\bar{\sigma}} [|U_x^\sigma(\mathbf{r})|^{-1} + |U_x^{\bar{\sigma}}(\mathbf{r})|^{-1}]. \quad (26)$$

Equations (25) and (26) are proportionality relations that may be enforced *locally* in space [see Eqs. (27) and (28)]

below]. It is apparent that $z_{\sigma\sigma'}(\mathbf{r})$ set the characteristic sizes of the c-hole functions in terms of the sizes of the x-hole functions. The idea behind this assumption is the following: the smaller the x-hole around each electron is, the more tightly the electrons are screened. Therefore, they are expected to be correlated much less.

The above modeling provides¹²: (i) zero correlation energy for one-particle systems (as the exact one); (ii) exact short-range behavior of the λ -dependent c-hole functions; (iii) a “reasonable” decay in the limit $s \rightarrow \infty$; (iv) exact normalization of the λ -dependent c-hole functions. Furthermore, (v) $c_{\sigma\sigma'}$ can be defined in such a way that the total correlation energy of the 2DEG is exactly reproduced.¹³ As a result, when the (average) density has a realistic range, $0 < r_s = 1/\sqrt{\pi\rho} < 20$, we can use the following (approximate) parameterizations:

$$c_{\sigma\sigma}[r_s] = \alpha \log(r_s) + \beta r_s^\gamma \quad (27)$$

with $\alpha = -0.14151$, $\beta = 1.2261$, $\gamma = 0.14499$, and

$$c_{\sigma\bar{\sigma}}[r_s] = \delta r_s^\xi \quad (28)$$

with $\delta = 0.66325$ and $\xi = 0.12396$. When using the present correlation functional, the coefficients $c_{\sigma\sigma'}[r_s](\mathbf{r})$ must be calculated at each point in space by making use of the density, that is, $r_s(\mathbf{r}) = 1/\sqrt{\pi\rho(\mathbf{r})}$.

Here we propose a few simplifications along the lines of the previous sections. First, we may replace U_x^σ with an approximate expression obtained in Sec. II A. Secondly, we apply Eq. (6) to Eq. (24) leading to

$$D_\sigma(\mathbf{r}) \rightarrow \tilde{D}_\sigma(\mathbf{r}) = \pi\rho_\sigma^2(\mathbf{r}) + \frac{1}{6}\nabla^2\rho_\sigma(\mathbf{r}) - \frac{1}{8}\frac{(\nabla\rho_\sigma(\mathbf{r}))^2}{\rho_\sigma(\mathbf{r})}. \quad (29)$$

Now, conditions (i) and (ii) given above are no longer satisfied. The latter modification clearly affects the *same-spin* c-hole functions. Applying both of the described simplifications – which is naturally required in order to make the functional orbital-free – the correlation energy can be expressed in terms of the (spin-dependent) c-hole potentials, $U_c^{\sigma\sigma'}(\mathbf{r})$, as follows:

$$\tilde{E}_c^{\sigma\sigma'} = \frac{1}{2} \int d\mathbf{r} \rho_\sigma(\mathbf{r}) \tilde{U}_c^{\sigma\sigma'}(\mathbf{r}), \quad (30)$$

with

$$\begin{aligned} \tilde{U}_c^{\sigma\sigma}(\mathbf{r}) &= \frac{16}{81\pi} (8 - 3\pi) \tilde{D}_\sigma(\mathbf{r}) \tilde{z}_{\sigma\sigma}^2(\mathbf{r}) \\ &\times \left[2\tilde{z}_{\sigma\sigma}(\mathbf{r}) - 3 \ln \left(\frac{2}{3} \tilde{z}_{\sigma\sigma}(\mathbf{r}) + 1 \right) \right], \end{aligned} \quad (31)$$

and

$$\begin{aligned} \tilde{U}_c^{\sigma\bar{\sigma}}(\mathbf{r}) &= (2 - \pi) \rho_{\bar{\sigma}}(\mathbf{r}) \\ &\times [2\tilde{z}_{\sigma\bar{\sigma}}(\mathbf{r}) - \ln(2\tilde{z}_{\sigma\bar{\sigma}}(\mathbf{r}) + 1)], \end{aligned} \quad (32)$$

where $\tilde{z}_{\sigma\sigma'}(\mathbf{r})$ are obtained by replacing U_x^σ with \tilde{U}_x^σ in Eqs. (25) and (26).

III. TESTING THE MODIFICATIONS

Next we test the modifications for different 2D quantum-dot systems. As a standard test set we consider parabolic (harmonic) dots consisting of N electrons confined in an external potential $v_{\text{ext}}(r) = \omega^2 r^2/2$. First we use the `octopus` code³¹ to solve the KS problem self-consistently using the exact-exchange (EXX) functional within the Krieger-Li-Iafrate (KLI) approximation.³² Then the resulting KS orbitals – and for the modified functionals solely the electron density and its gradients – are used to compute the energy expressions and their ingredients introduced in the previous sections. The obtained exchange energies can be directly compared with the EXX-KLI results E_x^{EXX} . In addition to this test set, we also consider a large quantum dot where we compare with the LSDA, as well as a rectangular quantum slab. In the case of correlation, we exploit the numerically exact configuration-interaction data³³ for the total energies $E_{\text{tot}}^{\text{ref}}$, so that the reference correlation energy can be evaluated from $E_c^{\text{ref}} = E_{\text{tot}}^{\text{ref}} - E_{\text{tot}}^{\text{EXX}}$.

A. Exchange energies

First we test the ingredients entering in the expressions for the exchange energy in Secs. II A and II B.

Figure 1(a) shows the original and modified kinetic-energy densities [as defined in Eq. (6)] of a spin-polarized three-electron parabolic quantum dot with $\omega = 1/4$. The characteristic step in τ_σ at the shell of the quantum dot at $r \sim 3$ is significantly smoother in $\tilde{\tau}_\sigma$. However, this difference is partly washed away in the local curvature of the x-hole shown in Fig. 1(b).

In the exchange-hole potential shown in Fig. 2(a) – computed with the functional described in Sec. II B – the difference is reduced further, so that the results are almost identical. Moreover, they agree very well with the EXX-KLI result corresponding to the Slater potential (dotted line). Naturally, this similarity leads to precise exchange energies as explicitly shown below.

In Fig. 2(b) we show the exchange-hole potentials calculated with the functional described in Sec. II B. Again, the results with and without the modification of the functional are similar, although the relative difference is larger than in the previous case [Fig. 2(a)]. Both potentials, however, deviate rather strongly from the EXX-KLI result. This tendency is already present in the original functional, which has been tailored mainly to produce accurate exchange *energies*,¹¹ which is indeed the case as shown below.

Table I shows the exchange energies calculated for several quantum dots. The set includes four cases with orbital currents (rows 1, 3, 4, and 7), in two cases arising from an external magnetic field perpendicular to the 2D plane (rows 3 and 7).³⁴ We consider modifications for both E_x^{model} and E_x^{1BSDM} , respectively. Overall, the modifications preserve the excellent performance of the

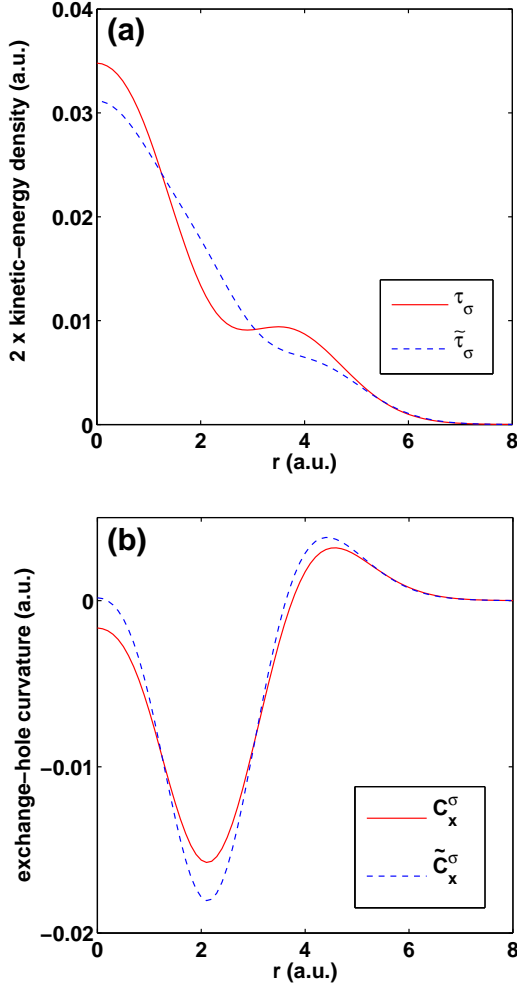


FIG. 1: (color online) (a) Comparison of the original (solid line) and modified (dashed line) kinetic-energy density of a spin-polarized three-electron parabolic ($\omega = 1/4$) quantum dot. (b) Local curvature of the exchange hole calculated from the original (solid line) and modified (dashed line) kinetic-energy density.

functionals very well (see the last row of Table I). For the 1BSDM approximation the modification even improves the performance. The LSDA is giving clearly the worst accuracy of the tested functionals.

In addition to the test set of Table I that covers only few-electron quantum dots, we now consider two rather different cases. First we focus on a large 48-electron parabolic quantum dot with $\omega = 0.3373$ at a magnetic field of $B = 3.05$ T. This partially spin-polarized (total spin $S = 3$) ground state has a compact “spin droplet” on the second-lowest Landau level, and its existence has been confirmed in recent spin-blockade experiments.^{35,36} Here we have performed a LSDA calculation and use that density as an input in the functionals. Figure 3 shows the kinetic-energy densities and exchange-hole potentials calculated with the functionals obtained from the modeling of the exchange hole (see Sec. II A). The orig-

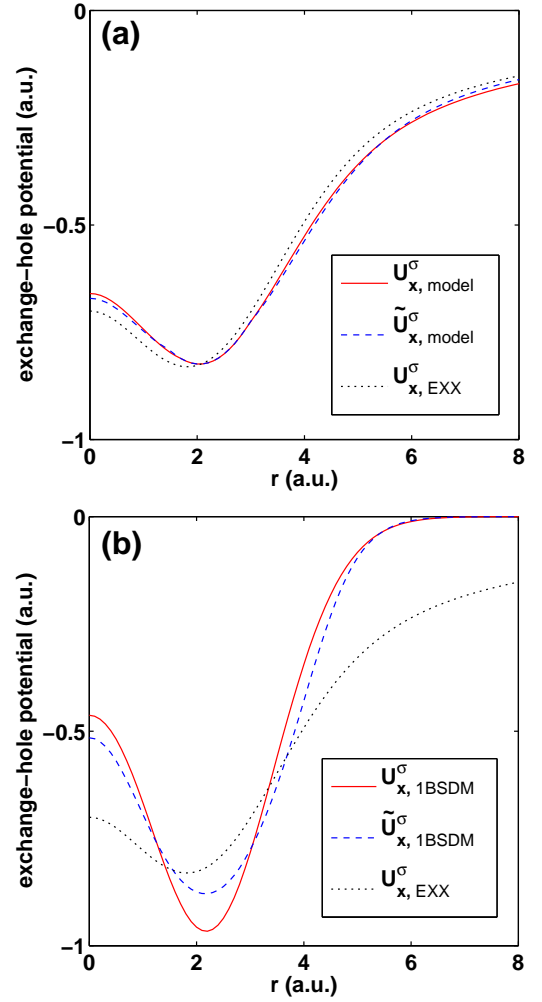


FIG. 2: (color online) Exchange-hole potentials of a spin-polarized three-electron parabolic ($\omega = 1/4$) quantum dot. (a) Result of the functionals in Ref. 9 without (solid line) and with (dashed line) the modification (see Sec. II A). (b) The same as (a) for the functional in Ref. 11 (see Sec. II B). The dotted line corresponds to the EXX-KLI result.

inal and modified τ_σ for both spin-up and spin-down electrons are very similar, and the resulting exchange-hole potentials are practically the same. The exchange energies are $E_x^{\text{model}} = -22.18$ and $\tilde{E}_x^{\text{model}} = -22.25$ (difference of 0.3%). In comparison, the LSDA yields $E_x^{\text{LSDA}} = -21.11$. In lack of a reliable EXX reference result for a system of this size it is not possible to judge whether the exchange energy from the model(s) or from the LSDA is more accurate. However, knowing that the LSDA typically underestimates the (absolute value of) E_x , our results for E_x^{model} and $\tilde{E}_x^{\text{model}}$ deviate from the LSDA in the correct direction. Most importantly, the exchange-hole potentials from the model are more accurate, especially in the asymptotic region.⁹

Our second example of a quantum-dot system that differs from those in Table I is a 16-electron rectangular hard-wall quantum slab with size $2\sqrt{2}\pi \times \sqrt{2}\pi$

TABLE I: Exchange energies for fully spin-polarized parabolic quantum dots calculated using the functional of Ref. 9 (E_x^{model}), its modification described in Sec. 2 ($\tilde{E}_x^{\text{model}}$), the functional in of Ref. 11 (E_x^{1BSDM}), its modification ($\tilde{E}_x^{\text{1BSDM}}$) described in Sec. II B, and the local spin-density approximation (E_x^{LSDA}). They are compared with the EXX-KLI result (E_x^{EXX}), so that the last row shows the mean absolute error in percentage.

N	$B(T)$	E_x^{model}	$\tilde{E}_x^{\text{model}}$	E_x^{1BSDM}	$\tilde{E}_x^{\text{1BSDM}}$	E_x^{LSDA}	E_x^{EXX}
2	0	-0.626	-0.634	-0.618	-0.620	-0.583	-0.626
3	0	-1.038	-1.043	-1.029	-1.021	-0.963	-1.021
3	2	-1.038	-1.056	-1.029	-1.037	-0.979	-1.039
4	0	-1.421	-1.435	-1.416	-1.408	-1.332	-1.374
5	0	-1.865	-1.876	-1.846	-1.842	-1.745	-1.816
6	0	-2.267	-2.275	-2.249	-2.241	-2.126	-2.214
6	3	-2.349	-2.391	-2.344	-2.362	-2.241	-2.357
		1.5	2.4	1.4	0.9	4.9	

corresponding to $\sim 90 \text{ nm} \times 45 \text{ nm}$ in SI units.³⁴ In Fig. 4 we compare the exchange-hole potentials given by the 1BSDM functionals (see Sec. II B) to the EXX-KLI (Slater) potential computed. The overall shapes are very similar, but as expected, the EXX-KLI potential is considerably smoother. Interestingly, however, the modified potential is qualitatively closer to the EXX-KLI result than the original one. Regarding the exchange energies both functionals perform similarly: $E_x^{\text{1BSDM}} = 13.13$, $\tilde{E}_x^{\text{1BSDM}} = 13.15$, and $E_x^{\text{EXX}} = 12.7$. Thus, the modification in τ_σ is well justified also when considering a 2D system with a hard-wall geometry.

B. Correlation energies

Figure 5 shows the spin-pair components of the correlation-hole potentials for a spin-unpolarized (total spin $S = 0$) six-electron parabolic quantum dot ($\omega = 1/4$) calculated with the model of Ref. 13 in comparison with its modifications introduced in Sec. II C. The modification induces clear deviations from the original potential, especially for the same-spin component affected by modifications in D_σ . For example, the bump at $r \sim 4$ is due to the change of sign in \tilde{D}_σ in that regime. In contrast, the opposite-spin component is independent of D_σ [see Eq. (32)], so that the modified functionals are almost the same; here the choice of $\tilde{U}_{x,\text{model}}^\sigma$ instead of $U_{x,\text{EXX}}^\sigma$ has a negligible effect (solid and dashed lines overlap). In lack of an *exact* reference result we cannot assess the quality of the correlation-hole potential(s). Hence, in the following we will focus on the correlation energies for which reference results can be obtained as described in the beginning of Sec. III.

In Table II we test the effect of the modifications for the accuracy of the correlation-energy functional. As discussed at the end of Sec. II C, we consider two approxi-

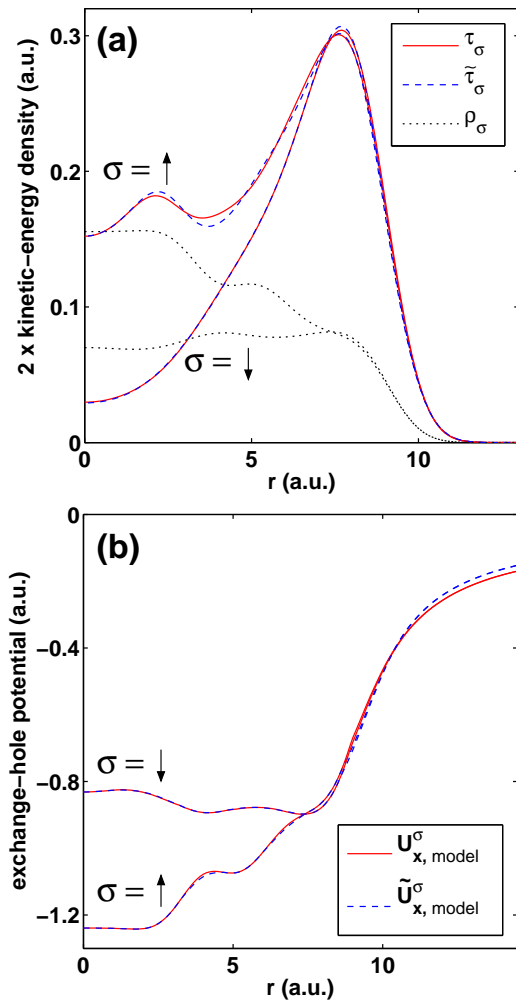


FIG. 3: (color online) (a) Original (solid lines) and modified (dashed lines) kinetic-energy densities for spin-up and spin-down electrons in a 48-electron parabolic ($\omega = 0.3373$) quantum dot at $B = 3.05$ T. The dotted lines show the spin densities. (b) Resulting spin-up and spin-down exchange-hole potentials using the functionals obtained from the modeling of the exchange hole (see Sec. II A).

mations, where we either do *not* approximate U_x in the same framework but use the EXX result, or then we apply the modification also to U_x . Interestingly, the best result – apart from the original functional which is very close in accuracy – is given by $\tilde{E}_c(\tilde{U}_x^\sigma)$ for both spin-polarized and unpolarized cases. This finding may demonstrate the compatibility between the corresponding exchange- and correlation-energy functionals. Nevertheless, all the functionals introduced here are superior to the LSDA, whose error is an order of magnitude larger.^{12,13}

Finally, in Fig. 6 we plot the relative errors of the correlation-energy functionals as a function of N (cf. Fig. 2 in Ref. 13). It is interesting to note that, at least for this set of systems, the modified functionals show consistent behavior as a function of the number of electrons. Thus, it may be expected that the good performance continues

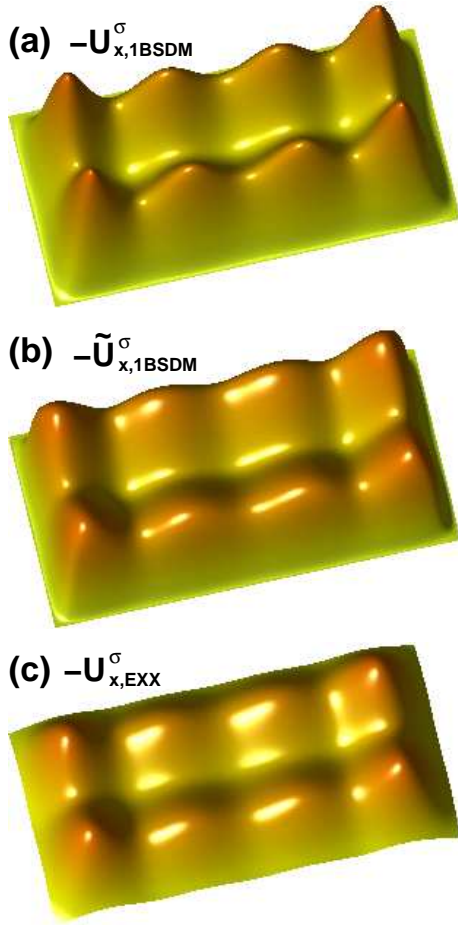


FIG. 4: (color online) Exchange-hole potentials of a 16-electron rectangular quantum dot calculated with the original (a) and modified (b) functionals obtained from the one-body spin-density matrix (see Sec. II B) in comparison with the exact-exchange (Slater) potential (c).

further to larger N . Unfortunately, a throughout testing of this is beyond the capability of numerically exact methods to provide accurate reference data.

IV. CONCLUSIONS AND OUTLOOK

In this work we have explored the possibility to modify meta-generalized-gradient approximations (meta-GGAs) for the exchange and correlation energies of two-dimensional systems to Laplacian-level meta-GGA ones. We have analyzed the effects of the according modifications on various systems. Although the differences in the kinetic-energy densities can be considerable, the functionals considered in this work preserve well the quality of the exchange- and correlation-hole potentials, and in particular the corresponding energies. Overall, we find that the performance is well preserved, if not even improved, by the modifications.

The simplified meta-GGAs provide significant prac-

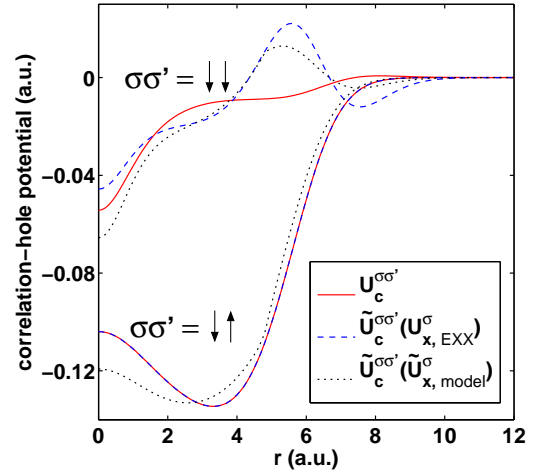


FIG. 5: (color online) Spin-pair components of the correlation-hole potential for a spin-unpolarized six-electron parabolic ($\omega = 1/4$) quantum dot calculated using the functional obtained from the correlation-hole modeling¹³ (solid line), its modification described in Sec. II C with $U_{x,EXX}^\sigma$ (obtained within the KLI approximation) as an input (dashed line), and with $\tilde{U}_{x,model}^\sigma$ as an input (dotted line).

TABLE II: Correlation energies for spin-polarized ($S = N/2$) and unpolarized ($S = 0$) parabolic quantum dots calculated using the functional in Ref. 13 (see Sec. II C), its modification with $U_{x,EXX}^\sigma$ (in the KLI approximation) as an input, the modified form with \tilde{U}_x^σ as an input, and the local-spin-density approximation.³⁷ The last column shows the numerically exact reference result. The last row shows the mean absolute error in percentage.

N	S	ω	E_c	$\tilde{E}_c(U_{x,EXX}^\sigma)$	$\tilde{E}_c(\tilde{U}_{x,model}^\sigma)$	E_c^{LSDA}	E_c^{ref}
2	1	1/4	-0.0115	-0.0073	-0.0085	-0.0345	-0.0100
3	3/2	1/4	-0.0225	-0.0189	-0.0200	-0.0564	-0.0226
4	2	1/4	-0.0399	-0.0337	-0.0330	-0.0730	-0.0337
5	5/2	1/4	-0.0570	-0.0465	-0.0468	-0.0929	-0.0484
6	3	1/4	-0.0681	-0.0617	-0.0613	-0.1125	-0.0640
6	0	1/4	-0.390	-0.379	0.380	-0.458	-0.396
3	3/2	1/16	-0.0138	-0.0106	-0.0122	-0.0382	-0.0167
5	5/2	1/16	-0.0348	-0.0278	-0.0299	-0.0659	-0.0357
6	3	1/16	-0.0426	-0.0372	-0.0393	-0.0796	-0.0459
6	0	1/16	-0.228	-0.214	-0.220	-0.282	-0.250
			9.5	15	11	99	

ticality and numerical efficiency in the application of the functionals. Therefore, a self-consistent and multi-purpose implementation of the present toolbox of functionals is now within reach, enabling the investigation of (quasi-)two dimensional electronic nanostructures of experimental and technological relevance.

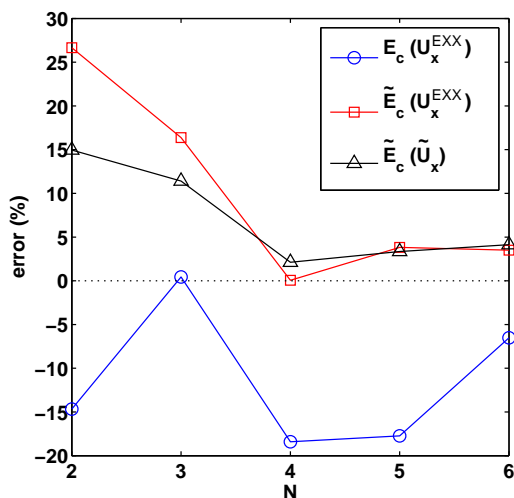


FIG. 6: (color online) Error in the correlation energy of spin-polarized parabolic ($\omega = 1/4$) quantum dots with N electrons obtained using different approximations. The circles correspond to the functional of Ref. 13 and the squares show the performance of the modified functional introduced in Sec. IIC, when the exact exchange-energy potential has been used in the expression. The triangles correspond to the case when also the exchange-energy potential has been used in a (similar) modified form.

Acknowledgments

This work has been supported by DOE grant DE-FG02-05ER46203 (S.P.) and by the Academy of Finland (E.R.).

-
- * Electronic address: pittaliss@missouri.edu
† Electronic address: erasanen@jyu.fi
- ¹ T. Ando, A. B. Fowler, and F. Stern, *Rev. Mod. Phys.* **54**, 437 (1982); L. P. Kouwenhoven, D. G. Austing, and S. Tarucha, *Rep. Prog. Phys.* **64**, 701 (2001); S. M. Reimann and M. Manninen, *Rev. Mod. Phys.* **74**, 1283 (2002).
 - ² G. F. Giuliani and G. Vignale, *Quantum Theory of the Electron Liquid*, (Cambridge University Press, Cambridge, 2005).
 - ³ R. G. Parr and W. Yang, *Density-functional Theory of Atoms and Molecules* (Oxford University Press - New York, Clarendon Press, Oxford, 1989); R. M. Dreizler and E. K. U. Gross, *Density Functional Theory* (Springer, Berlin, 1990).
 - ⁴ J. P. Perdew and S. Kurth, *A Primer in Density Functional Theory*, Lecture Notes in Physics Vol. 620, edited by C. Fiolhais, F. Nogueira, and M. Marques (Springer, Berlin, 2003).
 - ⁵ Y.-H. Kim, I.-H. Lee, S. Nagaraja, J.-P. Leburton, R. Q. Hood, and R. M. Martin, *Phys. Rev. B* **61**, 5202 (2000).
 - ⁶ L. Pollack and J. P. Perdew, *J. Phys.: Condens. Matter* **12**, 1239 (2000).
 - ⁷ L. A. Constantin, *Phys. Rev. B* **78**, 155106 (2008).
 - ⁸ L. A. Constantin, J. P. Perdew, and J. M. Pitarke, *Phys. Rev. Lett.* **101**, 016406 (2008). See also erratum.
 - ⁹ S. Pittalis, E. Räsänen, N. Helbig, and E. K. U. Gross, *Phys. Rev. B* **76**, 235314 (2007).
 - ¹⁰ E. Räsänen, S. Pittalis, C. R. Proetto, and E. K. U. Gross, *Phys. Rev. B* **79**, 121305(R) (2009).
 - ¹¹ S. Pittalis, E. Räsänen, and E. K. U. Gross, *Phys. Rev. A* **80**, 032515 (2009).
 - ¹² S. Pittalis, E. Räsänen, C. R. Proetto, and E. K. U. Gross, *Phys. Rev. B* **79**, 085316 (2009).
 - ¹³ E. Räsänen, S. Pittalis, and C. R. Proetto, *Phys. Rev. B* **81**, 195103 (2010).
 - ¹⁴ S. Pittalis, E. Räsänen, and C. R. Proetto, *Phys. Rev. B* **81**, 115108 (2010).
 - ¹⁵ S. Pittalis, E. Räsänen, J. G. Vilhena, and M. A. L. Marques, *Phys. Rev. A* **79**, 012503 (2009).
 - ¹⁶ S. Pittalis, E. Räsänen, and M. A. L. Marques, *Phys. Rev. B* **78**, 195322 (2008).
 - ¹⁷ S. Pittalis and E. Räsänen, *Phys. Rev. B* **80**, 165112 (2009).
 - ¹⁸ A. K. Rajagopal and J. C. Kimball, *Phys. Rev. B* **15**, 2819 (1977).
 - ¹⁹ B. Tanatar, D. M. Ceperley, *Phys. Rev. B* **39**, 5005 (1989).
 - ²⁰ C. Attaccalite, S. Moroni, P. Gori-Giorgi, and G. B. Bachelet, *Phys. Rev. Lett.* **88**, 256601 (2002).
 - ²¹ J. P. Perdew and L. A. Constantin, *Phys. Rev. B* **75**, 155109 (2007).
 - ²² R. Sharp and G. Horton, *Phys. Rev.* **90**, 317 (1953).
 - ²³ J. D. Talman and W. F. Shadwick, *Phys. Rev. A* **14**, 36 (1976).
 - ²⁴ S. Kümmel, L. Kronik, *Rev. Mod. Phys.* **80**, 3 (2008).
 - ²⁵ E. Engel, *A Primer in Density Functional Theory*, Vol. 620 of *Lecture Notes in Physics*, edited by C. Fiolhais, F. Nogueira, and M. Marques (Springer, Berlin, 2003), p. 1.
 - ²⁶ T. Grabo, T. Kreibich, S. Kurth, and E. K. U. Gross, *Strong Coulomb Correlations in Electronic Structure Calculations: Beyond Local Density Approximations*, edited by V. Anisimov (Gordon and Breach, Amsterdam, 2000), p. 203.

- ²⁷ G. Vignale and M. Rasolt, Phys. Rev. Lett. **59**, 2360 (1987).
- ²⁸ G. Vignale and M. Rasolt, Phys. Rev. B **37**, 10685 (1988).
- ²⁹ K. Berkane and K. Bencheikh, Phys. Rev. A **72**, 022508 (2005).
- ³⁰ M. Brack and B. P. van Zyl, Phys. Rev. Lett. **86**, 1574 (2001).
- ³¹ M. A. L. Marques, A. Castro, G. F. Bertsch, A. Rubio, Comput. Phys. Commun. **151**, 60 (2003); A. Castro, H. Appel, M. Oliveira, C. A. Rozzi, X. Andrade, F. Lorenzen, M. A. L. Marques, E. K. U. Gross, and A. Rubio, Phys. Stat. Sol. (b) **243**, 2465 (2006).
- ³² J. B. Krieger, Y. Li, and G. J. Iafrate, Phys. Rev. A **46**, 5453 (1992).
- ³³ M. Rontani, C. Cavazzoni, D. Bellucci, and G. Goldoni, J. Chem. Phys. **124**, 124102 (2006).
- ³⁴ When transforming the (effective) atomic units given in the paper to SI units, we use the effective-mass approximation with the typical GaAs parameters: $m^* = 0.067 m_0$ and $\varepsilon = 12.4 \varepsilon_0$. Hence, the energies, lengths, and magnetic-field strengths scale as $E_h^* = (m^*/m_0)/(\varepsilon/\varepsilon_0)^2 E_h \approx 12 \text{ meV}$, $a_0^* = (\varepsilon/\varepsilon_0)/(m^*/m_0) a_0 \approx 10 \text{ nm}$, and $B_0^* = (m^*/m_0)^2/(\varepsilon/\varepsilon_0)^2 B_0 \approx 6.9 \text{ T}$, respectively. In the paper the magnetic fields are always given in Tesla for clarity.
- ³⁵ M. C. Rogge, E. Räsänen, and R. J. Haug, Phys. Rev. Lett. **105**, 046802 (2010).
- ³⁶ E. Räsänen, H. Saarikoski, A. Harju, M. Ciorga, and A. S. Sachrajda, Phys. Rev. B **77**, 041302(R) (2008).
- ³⁷ Note that here the LSDA correlation energies have been calculated from the self-consistent EXX-KLI densities, whereas in Refs. 12 and 13 the LSDA correlation energies have been obtained self-consistently. The differences between the results are small.